Accepted Manuscript

Title: Endobronchial ultrasound-guided transbronchial needle aspiration in the diagnosis of mediastinal metastases of clear cell renal cell carcinoma

Authors: José-Fernando Val-Bernal, María Martino, Félix Romay, Elena Yllera

PII: S0344-0338(18)30027-X
DOI: https://doi.org/10.1016/j.prp.2018.05.021
Reference: PRP 52079

To appear in:

Received date: 9-1-2018
Revised date: 19-5-2018
Accepted date: 20-5-2018

Please cite this article as: José-Fernando Val-Bernal, María Martino, Félix Romay, Elena Yllera, Endobronchial ultrasound-guided transbronchial needle aspiration in the diagnosis of mediastinal metastases of clear cell renal cell carcinoma, Pathology - Research and Practice https://doi.org/10.1016/j.prp.2018.05.021

PRP_2018_27.R1

Endobronchial ultrasound-guided transbronchial needle aspiration in the diagnosis of mediastinal metastases of clear cell renal cell carcinoma

Running title:**EBUS-TBNA in mediastinal clear cell RCC**

José-Fernando Val-Bernal[a,*], María Martino[b], Félix Romay[c], Elena Yllera[d]

[a]*Pathology Unit, Medical and Surgical Sciences Department, University of Cantabria and IDIVAL Research Institute, Santander, Spain*

[b]*Anatomical Pathology Service, Marqués de Valdecilla University Hospital, University of Cantabria and IDIVAL Research Institute, Santander, Spain*

[c]*Neumology Service, Marqués de Valdecilla University Hospital, Santander, Spain,*

[d]*Radiodiagnostic Service, Marqués de Valdecilla University Hospital, Santander, Spain*

*Corresponding author at:

Pathology Unit, Medical and Surgical Sciences Department, University of Cantabria, Avda. Cardenal Herrera Oria s/n, 39011 Santander, Spain. E-mail address: fernando.val@unican.es (J.F. Val-Bernal).

ABSTRACT

Evaluation of mediastinal lymphadenopathy in patients with a previous diagnosis of renal cell carcinoma (RCC) is critical for the determination of further treatment. A minimally invasive method of cytology sampling of mediastinal lymph nodes using endobronchial ultrasound-guided transbronchial needle aspiration (EBUS-TBNA) has emerged as a useful tool in diagnosis. Between January 2010 and April 2018, we performed 1,744 EBUS-TBNA studies of mediastinal and hilar lymph nodes for a variety of clinical indications including mediastinal malignancy. Sixteen patients (93.7% males, mean age 59.1 years, range 44-81 years) were diagnosed by cytological and cell block study to have metastatic clear cell RCC. Twelve patients had been diagnosed with clear cell RCC in the past (mean 39 months, range 4 to 89 months) while in four, the tumor was primarily diagnosed in the staging phase on the basis of EBUS-TBNA. The EBUS features of the mediastinal nodal masses included increase of size (mean 2.5 cm, range 1.6-3.8 cm), irregular, inhomogeneous, hypervascular, and hyperechoic echotexture. EBUS-TBNA is a procedure safe and effective for evaluating mediastinal lymphadenopathy in patients with clear cell RCC. Immunohistochemistry in the cell block is decisive for proper diagnosis. The cytologist plays a key role in the diagnosis of metastatic clear cell RCC due to the treatment implications that this neoplasm encompasses.

Keywords: Bronchoscopy, Mediastinal lymph node, Renal cell carcinoma, Ultrasound-guided cytology

1. Introduction

Renal cell carcinoma (RCC) is the third most common urologic neoplasm and accounts for about 5% of adult cancers in men and 3% in women [1]. The most common metastatic sites in order of frequency are lung, bone, lymph nodes, liver, adrenal, and brain [2].

Patients treated for RCC can subsequently develop one or several mediastinal lymphadenopathies. Furthermore, it has been demonstrated that RCC may metastasize to mediastinal lymph nodes without any abdominal lymph node involvement [3,4]. Exceptionally, mediastinal disease can be the initial manifestation of RCC [5-7]. Accurate pathological diagnosis of such mediastinal lesions is critical for effective treatment. Mediastinoscopy and open thoracic surgery are standard methods for mediastinal lymph node staging. However, they are invasive and costly, require general anesthesia, and complications cannot be ignored. Endoscopic ultrasonography-guided fine-needle aspiration (EUS-FNA) biopsy of mediastinal lymph nodes is a minimally invasive modality for tissue sampling of the mediastinum [8]. However, in terms of accessibility to some lymph nodes and of the amount of tissue that can be obtained, the procedure is limited.

Endobronchial ultrasound-guided transbronchial needle aspiration (EBUS-TBNA) cytology is a minimally invasive, safe and feasible procedure that can be used for diagnosing mediastinal lymphadenopathy [9]. There are reports of isolated cases [10,11] or small series [9] in the literature using this technique to detect metastatic RCC to the mediastinal lymph nodes.

In this study, we investigated the feasibility of EBUS-TBNA for evaluating mediastinal lymphadenopathy in clear cell RCC. Mediastinal lymph node metastases presented as a

recurrence or a primary diagnosis in a series of 16 patients diagnosed with clear cell (conventional) RCC.

2. Materials and methods

Between January 2010 and April 2018, we performed 1,744 EBUS-TBNA studies of mediastinal lymph nodes for a variety of clinical indications including mediastinal malignancy. In this study, EBUS-TBNA was used to assess mediastinal and hilar lymph nodes for the presence of metastatic clear cell RCC. All the cases were seen in-house. The lymph nodes sampled were enlarged (short axis > 1cm) according to computed tomography (CT) scans, and they were associated in some cases with nodular lesions in the lung.

Tumor staging was established according to the 7th edition of the AJCC Cancer Staging Manual [12]. Nuclear grade in the renal surgical specimens was established according to Fuhrman et al [13].

The determination of the suitability of the patient was made based on the location of the suspected nodal metastasis.

EBUS-TBNA was performed under local anesthesia and midazolam and fentanyl sedation as an outpatient procedure, using a flexible bronchoscope Olympus BF-UC160F-OL8 (Olympus, Tokyo, Japan) and an ultrasound image processor Olympus EUS Exera EU-c60 (Olympus, Tokio, Japan). Specimens were obtained with a 22-gauge needle. The average number of needle passes from each location was 3 (range 1-6).

An on-site evaluation was performed in all the cases and the specimen was deemed adequate. Each case had aspirate smears that were stained with Diff-Quick and Papanicolaou method. In all the cases we had cell block preparations. Sections of the cytoblocks were stained with hematoxylin and eosin. Immunopathological study was carried out on formalin-fixed 4-µm-thick paraffin-embedded tissue sections using the

EnVision FLEX Visualization System (Dako, Agilent Technologies, SL, Las Rozas, Madrid, Spain). Antibodies used in the immunohistochemical study are detailed in Table 1. The immunohistochemical reactions were performed using appropriate tissue controls. Automatic staining was accomplished on a Dako Omnis autostainer (Agilent Technologies, SL). Because of limited material and variation of the staining panel over the years, not all tumors were stained with the same series of antibodies.

3. Results

Over the study period (8 years and four months), we analyzed the data from 16 patients who underwent EBUS-TBNA with cytoblock. The patients underwent EBUS-TBNA because of suspected mediastinal metastasis according to CT. Twelve patients had been diagnosed with clear cell RCC in the past (mean 39 months, range 4 to 89 months) while in four, this tumor was primarily diagnosed in the staging phase by means of EBUS-TBNA (Table 2). At CT scan these four cases showed large, expansile, polylobulated, heterogeneous lesions due to internal necrosis and occasional calcifications. The peripheral areas were solid with mean density at the pre-contrast phase and intense contrast uptake at the cortico-medullary phase (Fig. 1). Perirenal adipose tissue invasion or renal sinus invasion was observed in all cases.

There were 16 (93.7%) male patients and the mean age was 59.1 years (range 44-81 years). The mean mediastinal lymph node size detected with CT and EBUS-TBNA was 2.5 cm (range 1.6-3.8 cm). Nine (52.6%) cases had solitary metastases in the mediastinum in absence of lung metastases. The interval to metastases varied from 0 to 89 months with a mean of 29.2 months.

CT-scans with contrast enhancement in 16 patients showed well-defined, large (Fig. 2A), heterogeneously enhancing

solid lesions with irregular central necrosis in the mediastinum (Fig. 2B and 2C). Some hyperenhancing lymph nodes simulated vascular structures. Reviewing the EUS features of the mediastinal nodal masses in these patients revealed that they were large (Fig. 2D), irregular, inhomogeneous, hypervascular, and mostly hyperechoic. No calcifications were seen in any of these lymph nodes.

Cytological smears showed a lymphoid and hemorrhagic background on which there were large, epithelioid cells arranged in flat cohesive sheets (Fig. 3A), small clusters (Fig. 3B) or scattered as isolated elements. Cellularity was low (20%) to moderate (80%). The cells had abundant cytoplasm and a centrally or eccentrically located round to slightly irregular nucleus. In most cases, these cells exhibited a visible or prominent nucleolus. Cytoplasms were translucent, vacuolated, or granular eosinophilic. Nuclear grooves or foamy cytoplasms were not seen. In some cases, the isolated tumor cells resembled macrophages. However, these cells did not show anthracotic pigment and presented nuclear atypia. Occasionally, the extensions showed groups of cartilaginous cells, bronchial glands or ciliated cells of the bronchial mucosa. All the patients were found to have cytological findings compatible with metastatic clear cell RCC.

The cell blocks showed fragments of tumor tissue (Fig. 4A). The neoplasms were constituted by polygonal cells limited by prominent sinusoidal vascular networks. The observed architectural patterns were: solid nests (81.2%), alveoli (12.5%), and enlarged vascular spaces (6.2%). Cells were large and separated from one another by well-defined cell borders. These cells often had clear moderate to voluminous cytoplasm (Fig. 4B). Others showed fine granular, acidophilic cytoplasm. All tumors contain clear cells and a variable proportion of cells with eosinophilic cytoplasm

(Fig. 4C). Predominance of eosinophilic cells was observed in 81% (13/16) of tumors. Nuclei tended to be round to oval, and uniform with granular evenly distributed chromatin. Depending upon the degree of differentiation nucleoli could be sparse, large or prominent and the nuclei markedly enlarged with irregular shapes, and pleomorphism. A poorly differentiated tumor showing hyperchromatic, pleomorphic nuclei and pink eosinophilic cytoplasm can be observed in Fig. 4D. The Fuhrman nuclear grades were not assessed in the tissue sections of the cytoblocks.

Immunohistochemical studies revealed reactivity of the tumor cells for RCC marker (13/15, 86.7%) (Fig. 5A), cluster of differentiation 10 (CD10, 12/14, 85.7%) (Fig. 5B), paired box 8 (PAX8, 14/14, 100%) (Fig. 5C), cytokeratin (CK) AE1/AE3 (15/15, 100%), epithelial membrane antigen (EMA, 15/15, 100%), carbonic anhydrase IX (CAIX, 12/12, 100%) (Fig. 5D), and vimentin (15/15, 100%). There was no reactivity for thyroid transcription factor-1 (TTF-1, 0/15, 0%), CK 7 (0/3, 0%), p63 (0/3, 0%) and p40 (0/3, 0%).

In the present study, there were no inadequate samples. No complications were observed in patients due to the use of the EBUS-TBNA procedure.

4. Discussion

Clear cell RCC is the most common variant of RCC accounting for about 75% of cases. The tumor typically develops during adulthood, with the incidence peaking during the sixth and seventh decades of life. The neoplasm occurs nearly twice as often in men as in women. Metastatic RCC is present in 25-30% of patients at diagnosis [14]. The tumor metastasizes to the lung through a hematogenous route. Metastases to the mediastinal lymph nodes are usually associated with lung metastases. Metastases to the mediastinal lymph nodes occur via a lymphogenous route from pulmonary metastatic lesions

including undetected micrometastasis. Other possible pathways include a lymphogenous route via the thoracic duct (through a retrograde flow) or the inferior pulmonary ligament (through the retroperitoneal lymphatics) [15]. Anyway, RCC rarely shows solitary mediastinal lymph node metastases without lung metastases [5-7,15].

In patients with mediastinal lesions and a past history of RCC, is crucial to distinguish metastatic recurrence from other causes of mediastinal lymphadenopathy such as tuberculosis, sarcoidosis, or lymphoma.

Radiologic diagnosis of lymph node involvement is based on morphologic criteria, especially increase in size observed at CT-scans. It is generally accepted that a normal lymph node has a maximum short-axis diameter of 10 mm or less [16]. However, about five percent of metastatic lymph nodes for RCC are smaller than 10 mm. In these cases the tumor invasion is microscopic. On the other hand, lymph nodes larger than 2 cm are almost always involved by metastases [17]. In addition, hypervascularity and inhomogeneous enhancement of enlarged lymph nodes should raise suspicion for malignant invasion [16]. The overall accuracy of lymph node staging by CT in RCC is reported to be between 83% and 89%. False-negative results caused by microscopic invasion occurs in 4-5% of cases [17].

It has been demonstrated that echofeatures alone are not reliable in determining the underlying etiology of the mediastinal lymphadenopathy [18]. Nevertheless, malignant mediastinal lymph nodes tend to be larger than non-malignant lymph nodes. Thus, larger lymph nodes in the elderly may carry a higher risk of malignancy and should undergo EBUS-TBNA.

Determining the primary location of the tumor based only on the cytology of metastatic lesions can be difficult in view

of the overlap in the morphology of different tumors such as carcinomas, melanomas, sarcomas, and lymphomas. Another factor is the variable origin of visceral clear-cell tumors from kidney, liver, adrenal, ovary, cervix, thyroid, breast, lung, alimentary tract, or salivary glands which increases the difficulty of identifying the primary site [19]. Therefore, EBUS-TBNA with the study of the cytoblock and the help of immunohistochemistry is especially useful in the evaluation of the mediastinum for suspected metastases. According to the International Society of Urologic Pathology Consensus Conference, PAX8 is the most useful marker for establishing the diagnosis of metastatic RCC, and CAIX is characteristically overexpressed in clear cell RCC in a membranous pattern [20]. In addition, clear cell RCC commonly express vimentin, epithelial markers such as CK AE1/AE3, CAM 5.2 and EMA, RCC marker and CD10. Vimentin is more intensely positive in high-grade tumors. RCC marker exhibits cytoplasmic and membranous positivity and its expression decreases with increasing grade. However, the fact that other tumors can express positivity for vimentin, epithelial markers, and CD10 limits their utility in difficult cases [20]. The most useful markers in the separation of clear cell from chromophobe RCC are CK7, RCC marker, CD10, vimentin, and CD117 [21].

On the other hand, immunohistochemistry is necessary in cases of high-grade, poorly differentiated tumors. In this context, the differentiation between urothelial carcinoma (UC) and clear cell RCC is critical. A panel highly sensitive for clear cell RCC includes vimentin, PAX8, CD10, and CAIX. The immunohistochemical profile of UC involves positivity for p63, CK7, INI-1, high molecular weight CK [22], or uroplakin II, GATA3, and p40 [23]. It should be noted that UC can be positive for PAX8 and CAIX in 17% and 33% of cases respectively [22].

Patients with isolated, asynchronous metastases in the mediastinal lymph nodes are amenable to a surgical resection. This treatment is safe, appears to extend survival, and should be considered an important component of treating patients with RCC who have asynchronous lymph node metastases [15,24,25].

Currently, National Comprehensive Cancer Network in the USA and European Association of Urology guidelines in Europe, emphasize the importance of clear cell histopathology versus non-clear cell histopathology as a key therapeutic decision point in the setting of stage IV (metastatic/unresectable, or metastatic recurrent) RCC [26,27]. Thus, PAX8 plus CAIX expression not only establishes a clear cell RCC diagnosis but also identifies a therapeutically actionable group for tyrosine-kinase inhibitors and/or potent immunotherapies that abrogate the PD-1 pathway [28]. Therefore, in this setting, the cytologist plays a key role in diagnosis and acquires a high degree of responsibility.

The complication rate for EBUS-TBNA is low and varies from 1.23% [29] to 1.44% [30]. They include device breakage, hemorrhage, pneumothorax, infections (mediastinitis, pneumonia, pericarditis, sepsis), and death (large cerebral infarction reported in one case) [29,30]. Regarding the benefits, EBUS-TBNA can reach multiple nodal stations, including the hilar lymph nodes. In addition, advantages such as adequacy assessment of the specimen, improved diagnostic yield, and reduction of additional procedures contribute to improving patient care [31].

In Conclusion, EBUS-TBNA is a minimally invasive procedure safe and feasible for evaluating mediastinal lymphadenopathy in patients with clear cell RCC. Immunohistochemistry in the cell block is definitive for precise diagnosis. The cytologist plays a key role in the diagnosis of metastatic

clear cell RCC due to the treatment implications that this neoplasm entails.

Compliance with ethical standards

This study was approved by the Ethics Committee of IDIVAL Research Institute (CI: 2018.020) and confirmed to the provisions of the Declaration of Helsinki

Conflict of interest

The authors declare no conflict of interest.

Funding

No external funding for this work

References

[1] R.L. Siegel, K.D. Miller, A. Jemal, Cancer statistics, 2017, CA. Cancer J. Clin. 67(2017)7-30.

[2] M. Bianchi, M. Sun, C. Jeldres, S.F. Shariat, Q.D. Trinh, A. Briganti, Z. Tian, J. Schmitges, M. Graefen, P. Perrote, M. Menon, F. Montorsi, P.I. Karakiewicz, Distribution of metastatic sites in renal cell carcinoma: a population-based analysis, Ann. Oncol. 23(2012)973-980.

[3] K. Yamashita, M. Yamamoto, H. Nishimura, H. Akiyama, E. Tsuchiya, S. Tanaka, Hilar lymph node metastasis in renal cell carcinoma, Jpn. J. Thorac. Cardiovasc. Surg. 48(2000)194-197.

[4] K. Miyakazi, S. Sato, T. Kodama, K. Kurishima, H. Satoh, N. Hizawa, Mediastinal lymph node metastasis of renal cell carcinoma: a case report, Oncol. Lett. 11(2016)1600-1602.

[5] J. Mattana, B. Kurtz, A. Miah, P.C. Singhal, Renal cell carcinoma presenting as a solitary anterior superior mediastinal mass, J. Med. 27(1996)205-210.

[6] S. Moriyama, M. Yano, H. Haneda, K. Okuda, O. Kawano, Y. Hikosaka, R. Oda, A. Suzuki, R. Nakanishi, Solitary metastasis from renal cell carcinoma in the anterior mediastinal lymph node, Int. J. Clin. Exp. Med. 9(2016)20345-20348.

[7] D. Merine, E.K. Fishman, Mediastinal adenopathy and endobronchial involvement in metastatic renal cell carcinoma, J. Comput. Tomogr. 12(1988)216-219.

[8] A. Fritscher-Ravens, P.V.J. Sriram, T. Topalidis, S. Jaeckle, F. Thonke, N. Soehendra, Endoscopic ultrasonography-guided fine-needle cytodiagnosis of mediastinal metastases from renal cell cancer, Endoscopy 32(2000)531-535.

[9] J. Park, S.J. Jang, Y.S. Park, Y.M. Oh, T.S. Shim, W.S. Kim, C.M. Choi, Endobronchial ultrasound-guided transbronchial needle biopsy for diagnosis of mediastinal lymphadenopathy in patients with extrathoracic malignancy, J. Korean Med. Sci. 26(2011)274-278.

[10] T. Nakajima, K. Yasufuku, M. Wong, A. Iyoda, M. Suzuki, Y. Sekine, K. Shibuya, K. Hiroshima, T. Iizasa, T. Fujisawa, Histological diagnosis of mediastinal lymph node metastases from renal cell carcinoma by endobronchial ultrasound-guided transbronchial needle aspiration, Respirology 12(2007)302-303.

[11] M. Evison, P.A.J. Crosbie, R. Booton, Thoracic metastasis from renal cell carcinoma. Bronchoscopic and EBUS images, J. Bronchol. Intervent. Pulmonol. 22(2015)55-57.

[12] P. Rubin, J.T. Hansen, TNM Staging Atlas with Oncoanatomy, 2nd edition, Wolters Kluwer/Lippincott Williams & Wilkins, Philadelphia, 2012.

[13] S.A. Fuhrman, L.C. Lasky, C. Limas, Prognostic significance of morphologic parameters in renal cell carcinoma, Am. J. Surg. Pathol. 6(1982)655-663.

[14] R.J. Motzer, N.H. Bander, D.M. Nanus, Renal-cell carcinoma, N. Engl. J. Med. 335(1996)856-875.

[15] R. Kanzaki, M. Higashiyama, J. Okami, K. Kodama, Surgical treatment for patients with solitary metastasis in the mediastinal lymph node from renal cell carcinoma, Interact. Cardiovasc. Thorac. Surg. 8(2009)485-487.

[16] B. Paño Brufau, C. Sebastià Cerqueda, L. Buñesch Villalva, R. Salvador Izquierdo, B. Mellado González, C. Nicolau Molina, Metastatic renal cell carcinoma: radiologic findings and assessment of response to targeted

antiangiogenic therapy by using multidetector CT, RadioGraphics 33(2013)1691-1716.

[17] R.H. Reznek, CT/MRI in staging renal cell carcinoma, Cancer Imaging 4, Spec No A, (2004) S25-S32.

[18] L.H. Jamil, A. Kashani, D. Scimeca, M. Ghabril, S.A. Gross, H.R.S. Gill, M.K. Hasan, T.A. Woodward, M.B. Wallace, M. Raimondo M, Can endoscopic ultrasound distinguish between mediastinal benign lymph nodes and those involved by sarcoidosis, lymphoma, or metastasis? Dig. Dis. Sci. 59(2014)2191-2198.

[19] O. Nappi, S.E. Mills, P.E. Swanson, M.R. Wick, Clear cell tumors of unknown nature and origin: a systematic approach to diagnosis, Sem. Diagn. Pathol. 14(1997)164-174.

[20] V.E. Reuter, P. Argani, M. Zhou, B. Delahunt, and Members of the ISUP Immunohistochemistry in Diagnostic Urologic Pathology Group, Best practices recommendations in the application of immunohistochemistry in the kidney tumors. Report from the International Society of Urologic Pathology Consensus Conference, Am. J. Surg. Pathol. 38(2014)e35-e49.

[21] M, Zhou, A. Roma, C. Magi-Galluzzi, The usefulness of immunohistochemistry markers in the differential diagnosis of renal neoplasms, Clin. Lab. Med. 25(2005)247-257.

[22] J.C. Carvalho, D.G. Thomas, J.B. McHugh, R.B. Shah, p63, CK7, PAX8, and INI-1: an optimal immunohistochemical panel to distinguish poorly differentiated urothelial cell carcinoma from high-grade tumors of the renal collecting system, Histopathology 60(2012)597-608.

[23] L.L. Hoang, D. Tacha, R.E. Bremer, T.S. Haas, L.Cheng, Uroplakin II (UPII), GATA3, and p40 are highly sensitive markers for the differential diagnosis of invasive

urothelial carcinoma, Appl. Immunohistochem. Mol. Morphol. 10(2015)711-716.

[24] I. Takanami, M. Naruke, S. Kodaira, Long-term survival after resection of a mediastinal metastasis from a renal cell carcinoma, J. Thorac. Cardiovasc. Surg. 115(1998)1218-1219.

[25] B.A. Whitson, S.S. Groth, R. Andrade, L. Garrett, A.Z. Dudek, J. Jessurun, M.A. Maddaus, Extension of survival by resection of asynchronous renal cell carcinoma metastases to mediastinal lymph nodes, J. Thorac. Cardiovasc. Surg. 135(2008)1022-1028.

[26] T. Vermassen, A. De Meulenaere, M. Van de Walle, S. Rottey, Therapeutic approaches in clear cell and non-clear cell renal cell carcinoma, Acta Clin. Belg. 72(2017)12-18.

[27] B. Ljungberg, K. Bensalah, S. Canfield, S. Dabestani, F. Hofmann, M. Hora, M.A Kuczyk, T. Lam, L. Marconi, A.S Merseburger, P. Mulders, T. Powles, M. Staehler, A. Volpe, A. Bex, EAU guidelines on renal cell carcinoma: 2014 update, Eur. Urol. 67(2015)913-924.

[28] K.Y. Xu, S. Wu, Update on the treatment of metastatic clear cell and non-clear cell renal cell carcinoma, Biomark. Res. 3(2015)5.

[29] F. Asano, M. Aoe, Y. Ohsaki, Y. Okada, S. Sasada, S. Sato, et al., Complications associated with endobronchial ultrasound-guided transbronchial needle aspiration: a nationwide survey by the Japan Society for Respiratory Endoscopy, Respir. Res. 14(2013)50.

[30] G.A. Eapen, A.M. Shah, X. Lei, C.A. Jimenez, R.C. Morice, L. Yarmus, et al., Complications, consequences, and practice patterns of endobronchial ultrasound-guided

transbronchial needle aspiration. Results of the AQuIRE registry, Chest 143(2013)1044-1053.

[31] D. Jain, T.C. Allen, D.L. Aisner, M.B. Beasley, P.T. Cagle, V.L. Capelozzi, et al., Rapid on-site evaluation of endobronchial ultrasound-guided transbronchial needle aspirations for the diagnosis of lung cancer. A perspective from members of the Pulmonary Pathology Society, Arch. Pathol. Lab. Med. 142(2018)253-262.

Figure captions

Fig. 1. Thoraco-abdominal CT scan. Intravenous contrast in portal phase. Solid, exophytic, polylobulated mass located in the middle renal segment of the left kidney with a large hypodense central area of necrotic appearance (case 6). Image: (A) axial, (B) coronal, and (C) sagittal.

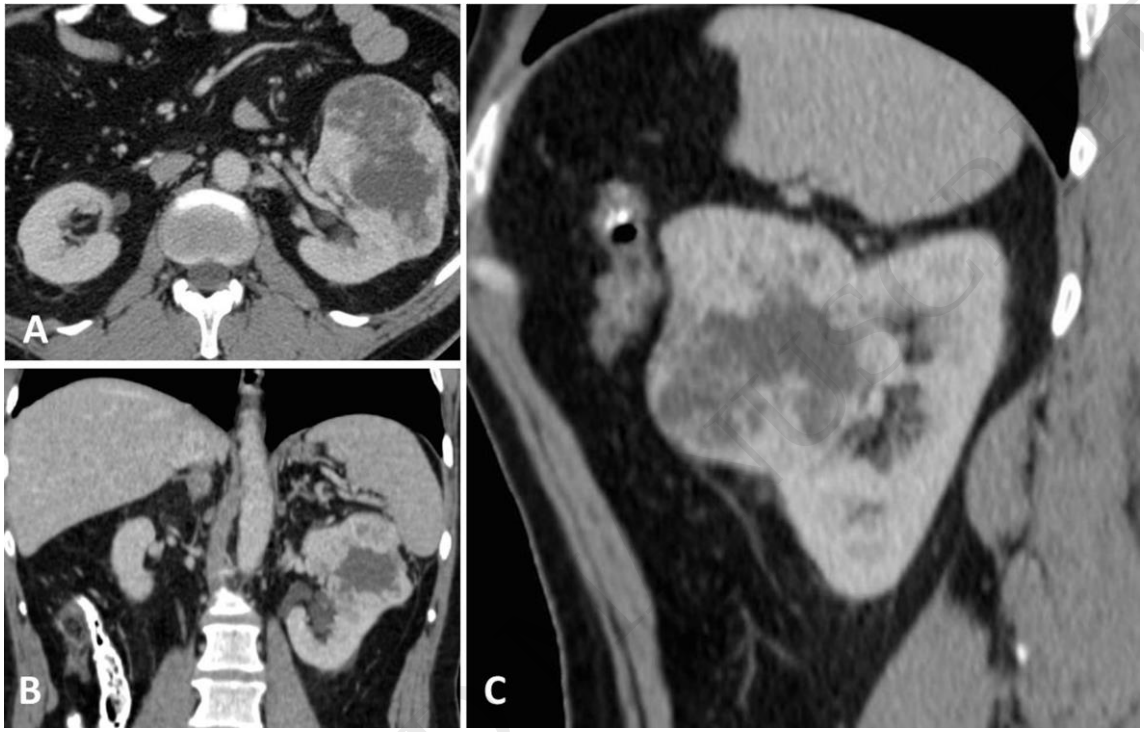

Fig. 2. Radiological findings. (A) Coronal thoracic CT scan. The arrow indicates an enlarged infracarinal lymphadenopathy (level 7). It is homogeneous, hypodense and rounded (case 11). (B) Axial thoracic CT image. The arrow points to an enlarged right hilar lymph node (10R), with a hypodense center suggestive of necrosis and with a polylobulated morphology (case 13). (C) Coronal thoracic CT scan. The arrow indicates a heterogeneous large lymph node in the most distal region of the left hilum (left interlobar, 11L). The hypodense internal areas suggest necrosis (case 14). (D) Endobronchial ultrasound image of an enlarged subcarinal lymphadenopathy (level 7) showing transbronchial needle aspiration (case 11).

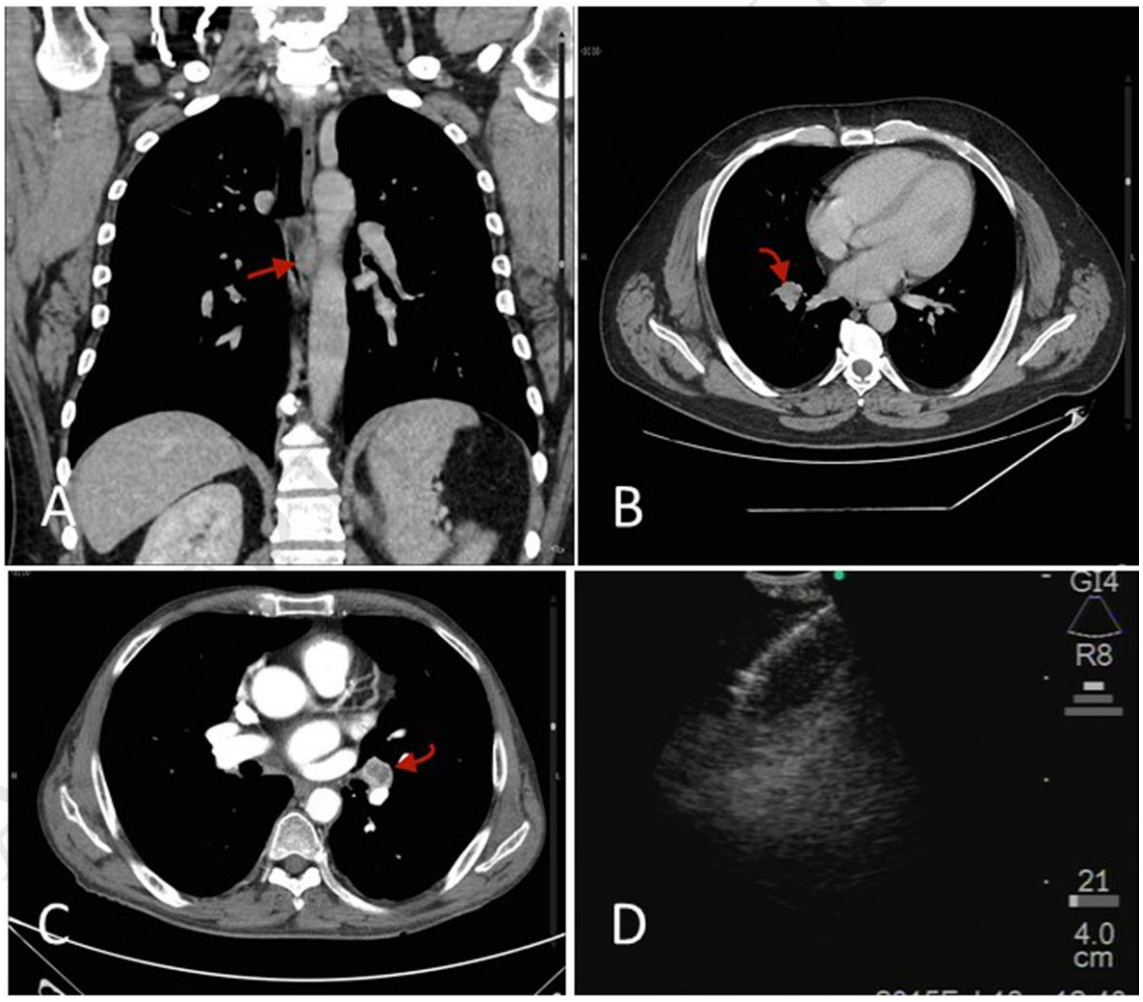

Fig. 3. Cytological smears. (A) Flat cohesive sheet of cells with abundant cytoplasm and a centrally or eccentrically located round to oval nucleus. Nucleoli are visible (case 4, Papanicolaou stain, x400). (B) Cytological smear showing a lymphoid and hematic background on which there is a group of large atypical cells with abundant cytoplasm and eccentrically located round nucleus (case 7, Diff-Quick stain, x400).

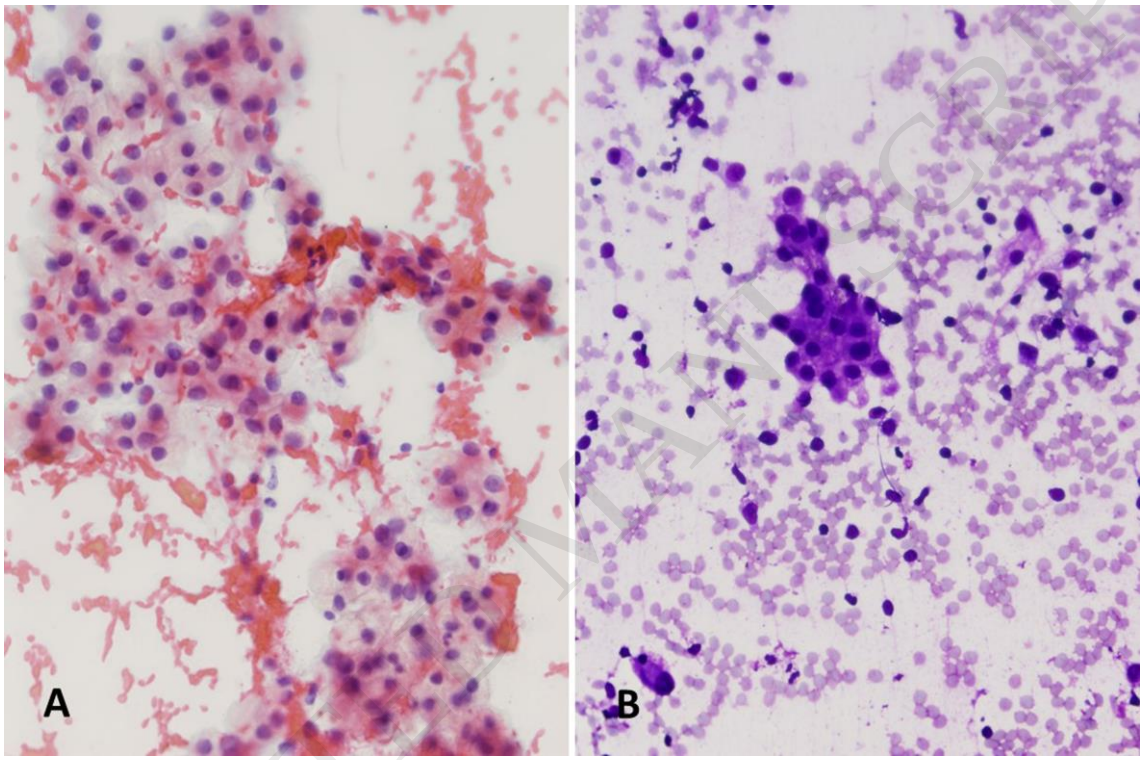

Fig. 4. Routine hematoxylin-eosin stain of the cell blocks. (A) Presence of tissue fragments of carcinoma cells in a background of red cells (Case 14, x100). (B) Solid architectural pattern of cells showing clear cytoplasm and distinct cell membranes (case 16, x400). (C) Tumor rich in cells with eosinophilic cytoplasm (case 14, x400). (D) Carcinoma cells displaying hyperchromatic and pleomorphic nuclei and eosinophilic cytoplasm (case 13, x400).

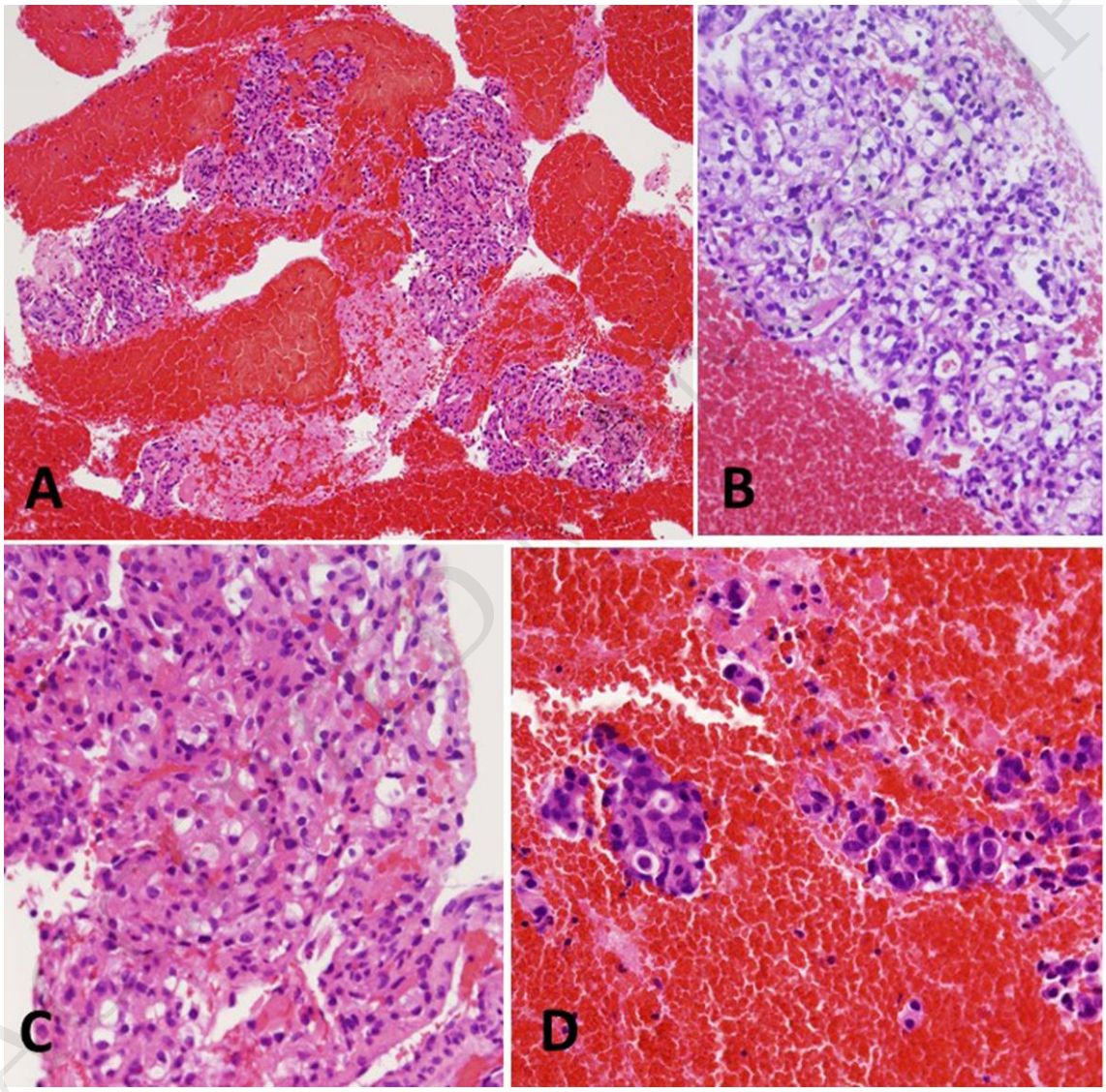

Fig. 5. Immunohistochemistry. Tumor cells show reactivity for: (A) renal cell carcinoma marker (case 8, x400), (B) CD10 (case 11, x400), (C) PAX8 (case 11, x400), and (D) CAIX (case 6, x400).

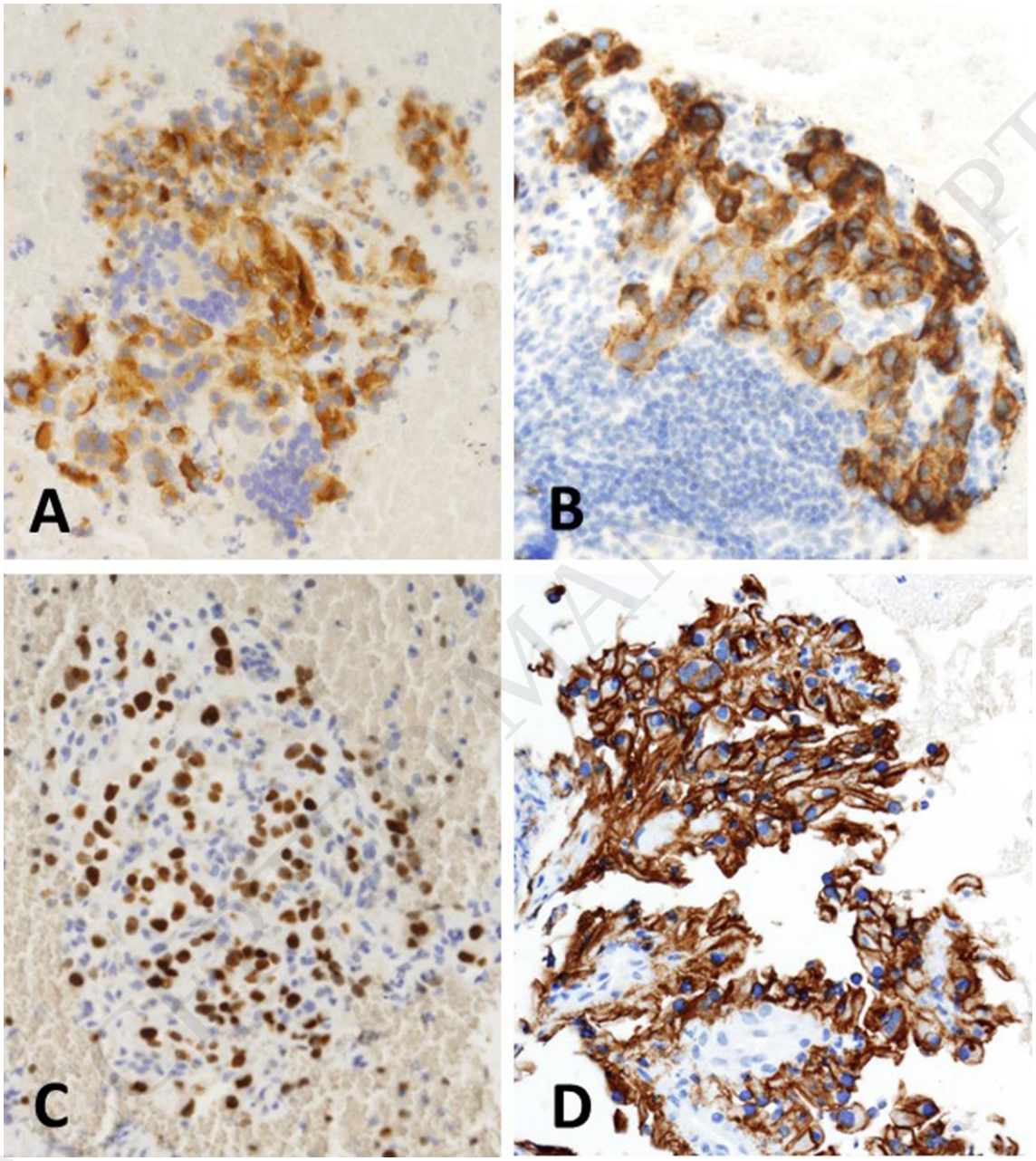

Table 1. Immunohistochemical antibodies used in the study

Antibody	Source	Clone	Dilution	Retrieval solution pH (Dako)
Renal cell carcinoma marker	Dako	SPM314	FLEX RTU	Low
CD10	Dako	56C6	FLEX RTU	Low
PAX8	Dako	Polyclonal	1:400	Low
TTF-1	Dako	8G7G3	FLEX RTU	High
Cytokeratin	Dako	AE1/AE3	FLEX-RTU	High
Epithelial membrane antigen	Dako	E29/EP1	FLEX-RTU	High
CAIX	Abcam	Polyclonal	1:1000	Low
Vimentin	Dako	V9	FLEX-RTU	High
Cytokeratin 7	Dako	OV-TL 12/30	FLEX-RTU	High
p63	Dako	DAK-p63	FLEX-RTU	High
P40	Biocare Medical	BC28	1:50	High

Dako (Agilent Technologies, SL, Las Rozas, Madrid, Spain); Abcam, Cambridge, United Kingdom; Biocare Medical, Alcalá de Henares, Madrid, Spain

Table 2. Clinical details of patients with mediastinal metastases caused by clear cell renal cell carcinoma

Case No	Age at metastases(y)/Sex	Thoracic imaging	Mediastinal lymph node máximum diameter (cm)	Previous tumor staging	Interval to metastasis (months)
1	50/M	Mediastinal lymph nodes Pulmonary nodes	2.9	pT2aN0M0,g3	16
2	62/M	Mediastinal lymph nodes Pulmonary nodes	2.5	pT3bN0M0,g2	72
3	49/F	Mediastinal lymph nodes Pulmonary nodes	2.0	pT2bN2M0,g3	4
4	69/M	Mediastinal lymph nodes Pulmonary nodes	3.5	pT4N0M1	26
5	57/M	Mediastinal lymph nodes	3.0	pT3bN0M0,g3	47
6	51/M	Mediastinal lymph nodes	1.6	pT3aN0M1,g3	0
7	74/M	Mediastinal lymph nodes	1.7	pT3aN0M0,g4	7
8	64/M	Mediastinal lymph nodes	2.4	T3N0M1	0
9	81/M	Mediastinal lymph nodes Pulmonary nodes	2.5	pT2aN0M0,g3	89
10	63/M	Mediastinal lymph nodes	3.5	pT2bN0M0,g3	55
11	44/M	Mediastinal lymph nodes	2.3	pT2aN0M0,g3	39
12	56/M	Mediastinal lymph nodes Pulmonary nodules	3.8	T3N2M1,g4	0
13	46/M	Mediastinal lymph nodes	2.0	pT3aN0M1,g4	0
14	56/M	Mediastinal lymph nodes	2.4	pT1bN0M0,g2	22
15	59/M	Mediastinal lymph nodes	1.7	pT3aN0M0,g2	24
16	65/M	Mediastinal lymph node Pulmonary nodules	2.0	pT1bpN0pM1,g3	67

g, Fuhrman grade